

High-temporal contrast using low-gain optical parametric amplification

Rahul C. Shah, Randall P. Johnson,* Tsutomu Shimada, Kirk A. Flipppo,
Juan C. Fernandez, and B. M. Hegelich

Los Alamos National Laboratory, Los Alamos, New Mexico 87545, USA

*Corresponding author: rpjohnson@lanl.gov

Received March 4, 2009; revised June 15, 2009; accepted June 22, 2009;
posted June 30, 2009 (Doc. ID 108372); published July 21, 2009

We demonstrate the use of low-gain optical parametric amplification (OPA) as a means of improving temporal contrast to a detection-limited level 10^{-10} . 250 μJ , 500 fs pulses of 1053 nm are frequency doubled and subsequently restored to the original wavelength by OPA with $>10\%$ efficiency. © 2009 Optical Society of America

OCIS codes: 190.4970, 230.4480, 170.7160, 140.3538.

Promising applications of relativistic light intensities achieved with terawatt chirped-pulse-amplification (CPA) lasers depend on the ability to control premature target ionization by preceding intensity spikes, compression quality, or amplified spontaneous emission (ASE). As an example, use of few-nanometers target foils in laser-based ion-acceleration schemes [1] with peak interaction intensities of 10^{20} W/cm² would require order 10^{-10} intensity contrast a few picoseconds from the peak. As laser powers grow, so too will the contrast requirement.

Since the strength of the ASE depends on the total gain it sees, one can meet the contrast requirement by inserting temporal cleaning subsequent to initial gain stages. If the pulse cleaner is placed between an additional compressor and stretcher, the technique is termed double-CPA [2]. Better ASE contrast requires positioning of the cleaning at later amplification stages.

Temporal cleaning using third-order nonlinear optics (χ^3) requires an intensity of order 10^{11} – 10^{12} W/cm² for efficient conversion. For the case of cross-polarization-wave generation [3], pulses >1 ps exceed the fluence damage of the crystal at this intensity. Access of χ^3 effects also brings about self-focusing effects that may degrade beam quality if applied in the near field, as higher power lasers will require.

Optical parametric amplification (OPA), a second-order nonlinear process (χ^2), in which a pump wave amplifies a lower-frequency signal and simultaneously generates an idler wave, offers an alternative using intensities of $\sim\text{GW}/\text{cm}^2$. In OPA, optical parametric noise (OPN) generates an incoherent background with temporal duration matching that of the pump. One approach for OPA application to contrast cleaning is to use a short-pulse pump laser that windows the gain. This has been experimentally demonstrated by using a pump duration <10 ps with approximately picosecond input [4]. Most recently, high-gain OPA with chirp compensation generated an ultrabroad bandwidth idler for which the combination of pump duration and chirp imply an OPN window <1 ps [5].

In this Letter we show that idler generation from low-gain OPA provides an insertable approach for improving temporal contrast. Working in the near field, 250 μJ , 500 fs pulses of 1053 nm are frequency doubled and subsequently restored to original wavelength by the OPA with $>10\%$ efficiency. Low-gain (2 – $20\times$) allows thinner crystals and minimizes bandwidth loss due to group-velocity mismatch (GVM). The results agree with expected temporal cubing of the input signal (within our 10^{-10} measurement limit), show stability on par with that of the input, and preserve spectral width and spatial quality.

The cubic relationship between the temporal profile of the idler and the signal is apparent from the OPA solution with undepleted pump approximation [6] and low gain. With I_i , I_s , and I_p referring to the idler, signal, and pump intensities respectively, linearizing the exponential gain (intensity gain <2) gives $I_i \propto I_{s0} I_p$. The cubic dependence occurs if the pump forms by doubling a portion of the original signal such that $I_p \propto I_s^2$. Regardless of larger gain or saturation effects, the conversion will fall into this cubic approximation in the temporal wings. From Manley–Rowe, the idler energy matches that added to the signal pulse. Assuming 50% doubling efficiency, picking off 10% of the initial energy as signal corresponds to an unsaturated gain of ~ 3 for complete pump extraction. For Type I phase matching, a slightly noncollinear geometry allows separation of the signal and idler, and for sufficiently small bandwidths angular dispersion can be neglected. Using high-quality surfaces, free propagation and a well-collimated beam minimizes scatter from the signal which would degrade the contrast.

Figure 1(a) presents the low-gain OPA pulse-cleaning scheme. A 90/10 beam splitter divides near-transform-limited 1053 nm, 500 fs pulses of up to 250 μJ . The larger portion frequency doubles by passing through 2 mm, Type I BBO with maximum efficiency near 70%. The s-polarized 527 nm light and the seed fundamental light then mix at $\sim 4^\circ$ (external angle) in an identical beta-barium-borate crystal for which an adjustable path allows temporal superposi-

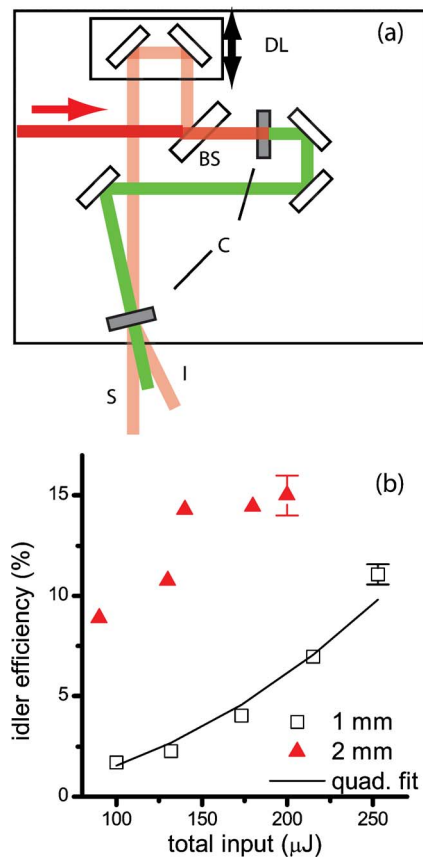


Fig. 1. (Color online) Schematic of low-gain OPA temporal pulse cleaning: DL, delay line; BS, 10/90 beam splitter; C, 2 mm Type I BBO crystal; S, signal; I, idler. (b) Idler efficiency for both 1 and 2 mm crystals.

tion. With $I_p \sim 4 \text{ GW/cm}^2$, the unsaturated gain measures 11. To demonstrate the scaling in the unsaturated regime, data using a 1 mm crystal is also presented. In the experiments with the thinner crystal we used slightly different experimental conditions than those detailed above. The pulses were not compressed to the transform-limited duration of 500 fs but instead were left partially chirped with duration $\sim 2 \text{ ps}$. Also, the mixing in the 1 mm crystal occurred at 10° , with diameter $\sim 1 \text{ mm}$, and used converging beams.

The scaling data are presented in Fig. 1(b) with representative measurement error bars. For the thinner crystal the measured efficiency fits a quadratic scaling for all data points with gain < 2 . In the case of the 2 mm crystal, the efficiency curve evidences strong saturation, which results in 1:1 relative stability between input and output. For the latter, the extraction efficiency of the pump reaches 50% and overall efficiency 15%.

A commercial third-order autocorrelator (Del Mar Photonics, San Diego) measured the temporal contrast with (idler) and without cleaning (signal with pump blocked) using $\sim 30 \mu\text{J}$. To create a fiducial, the beam passed a 5 mm etalon prior to the pulse-cleaning setup. The inset of Fig. 2(a) presents a 150 ps window, representative of longer scans (1 ns maximum). The first-order etalon reflection at 50 ps with intensity contrast 7×10^{-4} seen in the direct

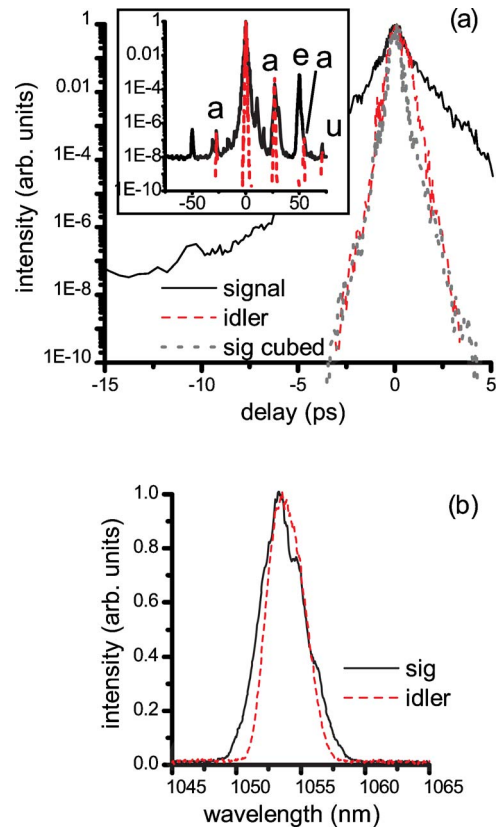


Fig. 2. (Color online) Temporal contrast measurement of both unamplified signal and idler with calculated cube of signal. Inset shows larger temporal range: a, known artifact; e, etalon reflection; u, unknown peak, presumed to be artifact. (b) Measured spectra.

measure of the regenerative amplifier appears in the idler scan as a peak of 4×10^{-10} . There is excellent agreement with the anticipated cubic relation, from which one expects an etalon peak of 3×10^{-10} in the cleaned pulse. As well, the ASE pedestal of contrast 10^{-8} and prepulse at -50 ps in the unamplified signal fall below the near- 10^{-10} detection limit of the device. In separate experiments we have measured scattering from the signal beam to be of order 10^{-4} into the $f/4$ collection at approximately the same separation angle [7]. Considering the diffraction-limited divergence, the collected scattering into the idler beam should reduce by an additional 10^{-5} . The net impact from scattering of a 10^{-3} reflection would then occur at 10^{-12} and that of the ASE at 10^{-17} . Several spikes occur identically in both cleaned and original pulses. Those labeled **a** correspond to first- and second-order reflections of the device filters. The origin of the post-pulse of strength 6×10^{-8} at 71 ps has not been identified.

The central image of Fig. 2(a) shows a temporal zoom of the inset and also includes the cubed contrast of the signal. Corrections for saturation do not improve the fit of the cube: its impact is small with respect to the steepness of the fall-off. Though the temporal cubing implies a $\sqrt{3}$ reduction in duration at the pulse peak, the durations appear equal. GVM in the cleaning may cause this, as calculated slip of the fundamental and harmonic is 140 fs [8] within each

2 mm crystal. Thus GVM becomes significant for pulses less than several hundred femtoseconds. The largest deviation from the fit occurs between 0.2 and 2.5 ps. As each measurement took on the order of 30 min, drift within the preceding stretcher and compressor can result in differing pulse shapes and durations. Several separate measurements support this explanation.

The spectra of both signal and idler are shown in Fig. 2(b). The cubic sharpening in the temporal domain corresponds to smoothing operations in frequency. Indeed, the discontinuities present in the signal spectrum are absent in the spectrum of the idler. The slight decrease (12%) in the spectral width could be attributed to GVM. In the experiments in which the input to the cleaning was partially chirped, we have observed spectral narrowing of the output, in agreement with the theory presented for a χ^3 process [9].

The final characterization essential for laser-chain implementation, that of near-field profile, is presented in Fig. 3. The beams fall directly upon the camera sensor at a distance ~ 1 m from the mixing. The images of (a) input signal and (b) idler clearly show that the OPA cleaning reduces the beam diameter [lineouts in (c)]. As expected, cubing of the input intensity occurs both in time and space. Reduction of the profile by $1.5\times$ indicates that saturation effects are minor and further supports the dominant role of GVM in filling out the temporal profile. Returning to Fig. 3, a second key point is the well-maintained quality of the near-field profile. At such low gains, some benefit may occur from the slight separation angle in the horizontal dimension as well as the

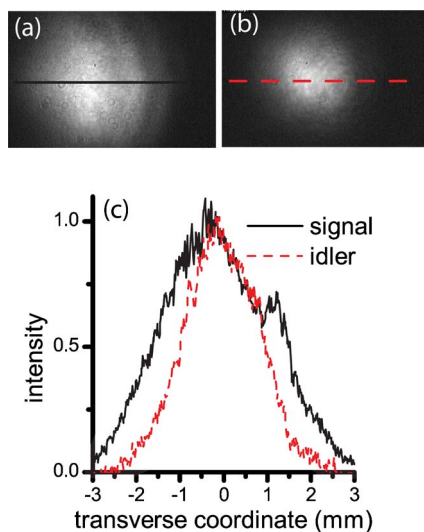


Fig. 3. (Color online) Near-field spatial profile of (a) unamplified signal and (b) idler.

Poynting walk-off in the vertical dimension, which result in profile shearing on the order 160 and $100\ \mu\text{m}$, respectively. As well, for low gain the idler retains the phase front of the input.

In summary we have presented the use of low-gain OPA as an insertable approach for temporal contrast improvement. The measured contrast improvement agrees well with expected temporal cubing, and we find better than 10% efficiency with $250\ \mu\text{J}$ input. Spectral width of the 500 fs pulse reduced only slightly, and the near-field mixing preserved the spatial quality. Cleaning of shorter pulse durations would require inclusion of techniques such as pulse tilting [10] or chirp compensation, which could obviate limitations of GVM in the existing configuration. Such techniques might also allow application of this scheme to larger beam apertures. We hope that along with its current application within an intense-laser chain [11], our presented findings will also benefit future systems requiring high temporal contrast.

Authors acknowledge support of U.S. Department of Energy (DOE) and Los Alamos National Laboratory Directed Research and Development. We acknowledge assistance of Trident and P-24 staff.

References and Notes

1. L. Yin, B. J. Albright, B. M. Hegelich, K. J. Bowers, K. A. Flippo, T. J. T. Kwan, and J. C. Fernández, *Phys. Plasmas* **14**, 056706 (2007).
2. M. P. Kalashnikov, E. Risse, H. Schönagel, and W. Sandner, *Opt. Lett.* **30**, 923 (2005).
3. A. Jullien, O. Albert, F. Burgy, G. Hamoniaux, J.-P. Rousseau, J.-P. Chambaret, F. Augé-Rochereau, G. Chériaux, J. Etchepare, N. Minkovski, and S. M. Saliel, *Opt. Lett.* **30**, 920 (2005).
4. C. Dorrer, I. A. Begishev, A. V. Okishev, and J. D. Zuegel, *Opt. Lett.* **32**, 2143 (2007).
5. Y. Tang, I. Ross, C. Hernandez-Gomez, G. New, I. Musgrave, O. Chekhlov, P. Matousek, and J. Collier, *Opt. Lett.* **33**, 2386 (2008).
6. A. Yariv and P. Yeh, *Optical Waves in Crystals* (Wiley & Sons, 1984).
7. R. C. Shah, R. P. Johnson, T. Shimada, and B. M. Hegelich, "Large temporal window contrast measurement using optical parametric amplification and low sensitivity detectors," *Eur. Phys. J. D* (to be published).
8. The SNLO nonlinear optics code is available from A. V. Smith at <http://www.sandia.gov/imrl/X1118/xxtal.htm>.
9. A. Jullien, L. Canova, O. Albert, D. Boschetto, L. Antonucci, Y.-H. Cha, J. Rousseau, P. Chaudet, G. Chériaux, J. Etchepare, S. Kourtev, N. Minkovski, and S. Saliel, *Appl. Phys. B* **87**, 595 (2007).
10. T. Zhang, H. R. Choo, and M. C. Downer, *Appl. Opt.* **29**, 3927 (1990).
11. R. P. Johnson, is preparing a paper to be titled "The enhanced Trident laser facility at the Los Alamos National Laboratory."